Ultrasound in Med. & Biol., Vol. 41, No. 5, pp. 1481–1487, 2015

0301-5629/$ - see front matter

http://dx.doi.org/10.1016/j.ultrasmedbio.2015.01.002

● *Technical Note*

WHAT DO WE KNOW ABOUT SHEAR WAVE DISPERSION IN NORMAL AND STEATOTIC LIVERS?

KEVIN J. PARKER,* ALEXANDER PARTIN,* and DEBORAH J. RUBENS†
*Department of Electrical & Computer Engineering, University of Rochester, Rochester, New York, USA; and †Department of Imaging Sciences, University of Rochester Medical Center, Rochester, New York, USA

(*Received* 12 *August* 2014; *revised* 29 *December* 2014; *in final form* 11 *January* 2015)

Abstract—A number of new approaches to measure the viscoelastic properties of the liver are now available to clinicians, many involving shear waves. However, we are at an early stage in understanding the physical processes that govern shear wave propagation in normal liver, with more unknowns added when pathologies such as steatosis are present. This technical note focuses on what is known about the characterization of normal and steatotic (or fatty) livers, with a particular focus on dispersion. Some studies in phantoms and mouse livers support the hypothesis that, starting with a normal liver, increasing accumulations of micro- and macrosteatosis will increase the lossy viscoelastic properties of shear waves in a medium. This results in an increased dispersion (or slope) of shear wave speed and attenuation in the steatotic livers. Theoretical and empirical findings across a number of studies are summarized.
(E-mail: kevin.parker@rochester.edu)

Key Words: **Liver, Ultrasound, Shear waves, Dispersion, Steatosis, Magnetic resonance elastography.**

INTRODUCTION

The accumulation of fat in the liver has important clinical consequences and is growing in prevalence. For example, non-alcoholic fatty liver disease (NAFLD) is an emerging national health problem, with an estimated prevalence of 23%–33.6% (Angulo 2002; Lam and Younossi 2010; Schreuder et al. 2008; Wanless and Lentz 1990). NAFLD is actually a higher risk factor for cardiovascular mortality and malignancy than for liver-related mortality (Ong et al. 2008). The risk factors for NAFLD (obesity and insulin resistance/type 2 diabetes) are increasing dramatically, and the incidences of NAFLD and NASH (non-alcoholic steatohepatitis) are rising proportionately. A significant fraction of people with NASH—between 20% and 40%—will develop progressive liver fibrosis (Dyson et al. 2014), leading to cirrhosis and increased risk of hepatocellular carcinoma.

Currently the only methods for quantitative measurement of steatosis are liver biopsy, which is invasive with concomitant patient risk, and magnetic resonance imaging (MRI), which is expensive and not widely available. Thus, there is need for a non-invasive and readily available method to quantify hepatic fat, which is a biomarker for hepatic disease and the metabolic syndrome. Most recent elastographic research and clinical studies have focused on liver fibrosis staging, which can be performed with several U.S. Food and Drug Administration-approved MRI and ultrasound imaging systems. In addition, transient elastography, which has no imaging component, is performed with the FibroScan instrument (Echosens, Paris, France) (Sandrin et al. 2003). Numerous studies have reported promising results for characterization of later-stage fibrosis (Bavu et al. 2011; Boursier et al. 2010; Huwart et al. 2008; Muller et al. 2009; Palmeri et al. 2008; Yin et al. 2007). The effect of steatosis on high-grade fibrosis measurement is not yet clear (Ferraioli et al. 2012). Compared with a larger body of studies of shear wave speed and fibrosis, relatively few studies have examined frequency-dependent shear wave properties, related to dispersion or viscoelastic models (Asbach et al. 2008; Bavu et al. 2011; Deffieux et al. 2015; Friedrich-Rust et al. 2009; Huwart et al. 2007; Klatt et al. 2007; Nightingale et al. 2013; Salameh et al. 2007; Wang et al. 2009). Nonetheless, there are some preliminary observations that can be made about dispersion measurements from lean and steatotic livers. Some theoretical considerations and then experimental

Address correspondence to: Kevin J. Parker, University of Rochester, Hopeman Building 203, PO Box 270126, Rochester, NY 14627-0126, USA. E-mail: kevin.parker@rochester.edu

results from the literature and across a number of different species and measurement techniques are presented in the next two sections.

THEORY

Theoretical basis

In an isotropic elastic medium, it can be shown that a rotational or shear wave can propagate with a speed $c_s = \sqrt{\mu/\rho}$, where μ is the shear modulus, and ρ is the density (Graff 1975). This equation is widely used in the field of elastography to connect an observed wave speed with the presumed tissue shear modulus and the related Young's modulus, assuming a nearly incompressible tissue with a density close to unity.

If the medium is not purely elastic, but also incorporates loss mechanisms, then an attenuation coefficient will be observed that increases with frequency, and the shear wave speed will also tend to increase with frequency. These increases with frequency are called attenuation dispersion and wave speed dispersion, respectively. The standard framework for this (Blackstock 2000; Carstensen and Parker 2014) begins with the plane wave solution for displacement, ξ,

$$\xi(x,t) = \xi_0 e^{j(\omega t - kx)} \tag{1}$$

where the wave number $k = \omega/\sqrt{\mu/\rho} = \omega/c_s$, and ω is frequency. The amplitude of the displacement ξ_0 is directly proportional to the applied surface stress. But if the wavenumber k is complex, then we can explicitly write the phase velocity and attenuation in terms of a complex shear modulus, $\mu = \mu_1 + j\mu_2$:

$$k = \beta - j\alpha = \frac{\omega}{\sqrt{\frac{\mu_1 + j\mu_2}{\rho}}} \tag{2}$$

Then,

$$\overrightarrow{\xi}(x,t) = \overrightarrow{\xi} e^{-\alpha x + j(\omega t - \beta x)} \tag{3}$$

Various models exist for the complex shear modulus; for example, in the simple Kelvin–Voigt model of a parallel spring and dashpot with viscosity η, the imaginary component μ_2 increases with frequency:

$$\mu = \mu_1 + j\omega\eta \tag{4}$$

Whereas for a linear hysteresis model, μ_2 is a constant H with respect to frequency:

$$\mu = \mu_1 + jH \tag{5}$$

Other models that may be relevant to soft tissues such as the liver are found elsewhere (Carstensen and Parker 2014; Klatt et al. 2007; Liu and Bilston 2000; Parker 2014; Zhang et al. 2007).

These various models, with the exception of linear hysteresis, predict that the complex modulus, and therefore the phase velocity, will increase with frequency, indicating a dispersive medium. Note that in a dispersive medium, the group velocity, which defines the speed of the envelope of a broadband signal, is different from the phase velocity (Fitzpatrick 2013).

Equation (2) illustrates a simple empirical fact: As the complex shear modulus μ_2 approaches zero, the imaginary part, and therefore the attenuation coefficient, approaches zero, and the wave speed becomes a constant (and independent of frequency) given by $\sqrt{\mu/\rho}$. Conversely, as the complex shear modulus increases from zero, the attenuation and wave number and phase velocity of the shear wave can increase with frequency; however, the exact form of the increase, which is the observed dispersion, depends on the nature of the loss element or the particular model used. Normal lean liver has a measurable shear wave attenuation and dispersion (data are provided in the next section), and the impact of early-stage steatosis is hypothesized to increase dispersion by the addition of a viscous material to the medium, in effect increasing μ_2 and therefore dispersion by eqns (2) and (3). However, finding the most appropriate physical model for this remains as an important research question. There is the additional possibility of attenuation losses caused by scattering from the fat-filled vacuoles in steatosis. Shear wave scattering theory is covered in Einspruch et al. (1960) and White (1958) and is complicated by mode conversion mechanisms. However, it remains to be seen how large a factor this may be in the common shear wave band of 40–1,000 Hz. Finally, it must be noted that the progression of lean liver to early-stage steatosis is marked by the accumulation of fat as macro- and microvesicles of triglycerides. This may be the simplest set of changes to model, as compared with cases with high-grade fibrosis, plus steatosis, plus other possible complications. It may be that an adequate model of dispersion from early-stage steatosis will not be adequate for a discussion of high-grade fibrotic or cirrhotic livers with steatosis.

Empirical basis

A number of different techniques and studies have been used to study steatosis in liver. In Figure 1 we attempt to plot on a common parameter space the results of a number of studies (Asbach et al. 2008; Barry et al. 2012, 2014a, 2014b; Bavu et al. 2011; Chen et al. 2009, 2013; Deffieux et al. 2009; Hah et al. 2012; Klatt et al. 2007; Muller et al. 2009; Orescanin and Insana 2010; Xie et al. 2010). All animal studies were performed in accordance with protocols approved by institutional committees on animal resources, and all human studies were performed in accordance with protocols approved

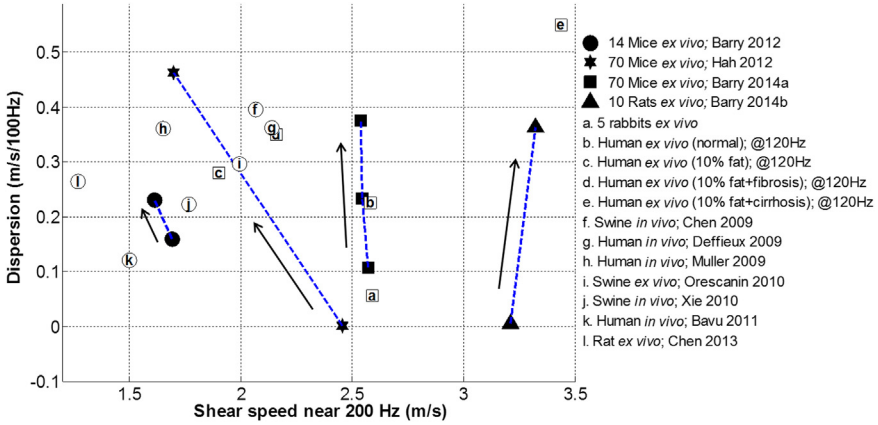

Fig. 1. Collected dispersion studies on lean or steatotic livers. The y-axis represents the dispersion in m/s per 100 Hz. The x-axis represents the shear speed at or near 200-Hz frequency (unless otherwise specified). The solid symbols represent lean-versus-steatotic comparison studies at the University of Rochester. For these four studies of lean versus steatotic livers, the *dotted lines* link the normal and steatotic liver groups for each study, and the *arrows* indicate the direction of increasing steatosis. *Solid squares* from Barry et al. (2014a) represent lean, medium-steatosis and high-steatosis groups. *Open squares a–e* are additional data from our lab derived from crawling wave measurements. *Open squares b–e* were reported in Barry et al. (2012). *Open circles f–l* represent data from other laboratories. A more detailed listing of experimental techniques, conditions of the livers and references is given in Table 1.

by institutional review boards. These studies were selected because they reported shear speed versus frequency data near 200 Hz, chosen as a common reference for which data are available from different reports. The vertical axis is the estimation of dispersion, or slope of the shear wave speed. The horizontal axis of Figure 1 is the reference shear wave speed found at or near 200 Hz. For studies in the literature in which the data were given graphically, we made a graphic estimate or extrapolation of these parameters. Other studies that directly fit their results to viscoelastic models are relevant, but do not appear in Figure 1 unless the raw dispersion data are published as well and are near 200 Hz (Asbach et al. 2008; Bavu et al. 2011; Friedrich-Rust et al. 2009; Klatt et al. 2007; Salameh et al. 2007, 2009).

Table 1 gives the conditions of the different studies, where known. The details of each experimental technique can be found in the individual references.

Generally, there is evidence across studies that lean livers (and presumed lean livers) have dispersions in the range of 0 to 0.4 m/s per 100 Hz, whereas steatotic livers have dispersions in the range of 0.2 to 0.5 m/s per 100 Hz. However, there is a wide range of estimated shear wave speed at the reference frequency near 200 Hz across the different measurements. Additional estimates from lower-frequency magnetic resonance elastography (MRE) experiments from the laboratory of Dr. I Sack are listed in Table 2. These show higher dispersion values, near 40 Hz, which may be consistent with some common viscoelastic models (Klatt et al. 2007). Some possible reasons for the range of values within Figure 1 are discussed in the next section.

DISCUSSION

The collected data cover a wide range of speed and dispersion (slope) values for lean livers. There are a number of experimental factors that would contribute to a wide range of estimated values, including technique differences, species differences, temperature differences and differences in the condition of the livers when the experiments were conducted. Many of these factors can be identified by reviewing Table 1. For example, experimental techniques range from sinusoidal steady-state shear waves to localized pulses from radiation force excitation. Species differences may play a role even in lean livers, as the lowest dispersion values across all studies come from leptin-deficient strains of young mice and rats examined by Barry et al. (2012, 2014a, 2014b). The condition of the livers at the time of measurement ranges from *in vivo* to *ex vivo*, in which case the effects of arterial pressure and body versus room temperature could result in variations. Furthermore, any long delays in the preparation and measurement of *ex vivo* samples could alter shear wave measurements as the liver will decompose over time. This could be a factor in the New Zealand White (NZW) rabbit livers which were refrigerated and stored for 1 day before measurements. They exhibit a relatively low dispersion given their average triglyceride level of 0.035 mg TG/mg liver.

The effects of temperature deserve additional focus, as so many laboratory studies on phantoms and tissues are conducted on *ex vivo* samples and over a potentially wide range of "ambient" temperatures. The theory of time–temperature superposition applies to the viscoelastic

Table 1. Parameters of liver dispersion studies

Reference/ study	Sample type	Method	Frequency range (Hz)	Dispersion (m/s/100 Hz)	Fat parameter	Temp (°C)	Imaging system; transducer
Barry et al. 2012	14 mice *ex vivo*	CrW	[100, 400]	Lean: 0.16 ± 0.03 Fatty: 0.23 ± 0.04	Diet type n = 7: regular diet n = 7: high-fat diet	~23	LOGIQ 9 (GE); M12L (GE)
Hah et al. 2012	70 mice *ex vivo*	CrW	[200, 350]	Group 1: ~0 Group 2: 0.46	Visual fat n = 51: fat (0, 50%) n = 14: fat (50, 90%)	~18.5	LOGIQ 9 (GE); M12L (GE)
Barry et al. 2014a	70 mice *ex vivo*	CrW	[200, 360]	Group 1: 0.11 Group 2: 0.23 Group 3: 0.38	TG per liver (mg/mg) n = 32: (0, 0.1) n = 21: (0.1, 0.25) n = 17: (0.25, 0.36)	17–19	Sonix Tablet (Ultrasonix); L40-8/12 Linear (Ultrasonix)
Barry et al. 2014b	10 rats *ex vivo*	CrW	[60, 260]	Group 1: ~0 Group 2: 0.36	TG per liver (mg/mg) n = 5: lean, avg: 0.0041 n = 5: fatty, avg: 0.0243	~18.5	LOGIQ E9 (GE); L8-18i-D (GE)
UR Study 5	5 NZW rabbits (obese) *ex vivo*	CrW	[110, 300]	0.06	TG per liver (mg/mg) avg: 0.0349	~18.5	LOGIQ 9 (GE); M12L (GE)
Barry et al. 2012	Four human samples *ex vivo*	CrW	[80, 180]	0.23; 0.28; 0.35; 0.55	Visual fat (%) Normal; 10%; 10% + fibrosis; 10% + cirrhosis	~23	LOGIQ 9 (GE); M12L (GE)
Chen et al. 2009 (Greenleaf)	Swine *in vivo*	SDUV	[100, 400]	0.40	NA	Body temp	Experimental
Deffieux et al. 2009 (Fink)	Three healthy human volunteers *in vivo*	SSI	[40, 450]	Average: 0.36	NA	Body temp	Research prototype (Supersonic Imagine); L7-4 (ATL Philips)
Muller et al. 2009 (Fink)	10 healthy human volunteers *in vivo*	SSI	[60, 390]	0.36 ± 0.08	NA	Body temp	Experimental
Orescanin and Insana 2010	Three fresh swine *in vitro*	Harmonic vibrations and Doppler scanning	[50, 300]	Average: 0.30	NA	23	SonixRP (Ultrasonix); BW 14/60 (Ultrasonix)
Xie et al. 2010 (Greenleaf and Philips)	Healthy farm swine *in vivo*	SDUV	[100, 400]	0.22	NA	Body temp	iU22 (Philips); C5-1 (Philips)
Bavu et al. 2011 (Fink)	Human *in vivo* (fibrosis stage F1); patient 111	SSI	[30, 435]	0.12	NA	Body temp	Supersonic Imagine; C4-2 (ATL)
Chen et al. 2013	Six rats *in vitro* (fibrosis stage F0)	SDUV	[100, 400]	Average: 0.26	NA	NA	SonixRP (Ultrasonix); L14-5 W (Ultrasonix)

CrW = crawling wave; SDUV = shear wave dispersion ultrasound vibrometry; SSI = supersonic shear imaging; TG = triglycerides; UR = University of Rochester.

behavior of polymers and biomaterials and has been used to explain the strong dependence of elasticity and shear wave speed on temperature (Chan 2001; Doyley et al. 2010). As an illustration of the major impact of "ambient" temperature on shear wave speed, Figure 2 provides measurements of shear wave speed versus frequency for a fresh bovine liver sample embedded in gelatin. These values were obtained with the "crawling wave" measurement approach used by Barry and coworkers (Barry et al. 2012, 2014a; Wu et al. 2004).

Table 2. Parameters of studies at lower shear wave frequencies

Reference/study	Sample type	Method	Frequency range (Hz)	Dispersion (m/s/100 Hz)	Fat parameter	Temp (°C)	Imaging system; transducer
Klatt et al. 2007 (Sack)	Healthy human liver *in vivo*	MRE	[25, 62.5]	0.752	NA	Body temp	1.5-T scanner (Magnetom Sonata; Siemens)
Asbach et al. 2008 (Sack)	Healthy human liver *in vivo*	MRE	[25, 62.5]	0.576	NA	Body temp	1.5 -T scanner (Magnetom Sonata; Siemens)

MRE = magnetic resonance elastography.

After the gelatin/liver sample was cooled to 4°C in a refrigerator, the crawling wave movies were obtained at discrete frequency at progressively increasing temperatures over the course of a few hours. Temperatures were monitored with a thermocouple placed near the center of the gelatin/liver specimen, but outside of the imaging plane. A roughly 3-cm lateral region of interest was used, and data points represent a single estimate on the imaged region of interest at a particular frequency. Consistent with earlier reports (Kruse et al. 2000; Sapin-de Brosses et al. 2010), the general trend is that colder samples are more "stiff" and have a higher shear wave speed than warmer temperatures, and even a few degrees Celsius difference will create a distinctly different set of shear wave speed estimates. The slope or dispersion in Figure 2 remains similar over this temperature range, which is consistent with time–temperature superposition (Chan 2001; Doyley et al. 2010) theory applied to a material with an extended range of relaxation functions (Zhang et al. 2007).

It should be noted that the rate of change of shear wave speed versus temperature is not strictly linear, as illustrated in Figure 3. However, as a general guideline, we have found that bovine liver and gelatin phantom results fall within a common range. To normalize the shear wave speed, we divide by the samples' speed at a reference temperature and frequency, such as 15°C at 150 Hz for convenience. Then the normalized change in shear wave speed per degree Celsius, $(\Delta c_s/c_{\text{ref}})/\Delta T$, is found to be in the range 0.025–0.040. In other words, for lean liver tissue or gelatin phantoms, one would expect an approximately 3% change in shear wave speed per degree Celsius as "ambient" temperature varies. This dependence on temperature may be higher in muscle tissue (Kruse et al. 2000; Sapin-de Brosses et al. 2010).

Finally, in assessing the spread of data in Figure 1, the two parameters of dispersion, (slope) and shear wave speed, have no obvious link across all the measurements. This can also be understood theoretically by assuming μ_1 and μ_2 are relatively independent in eqns

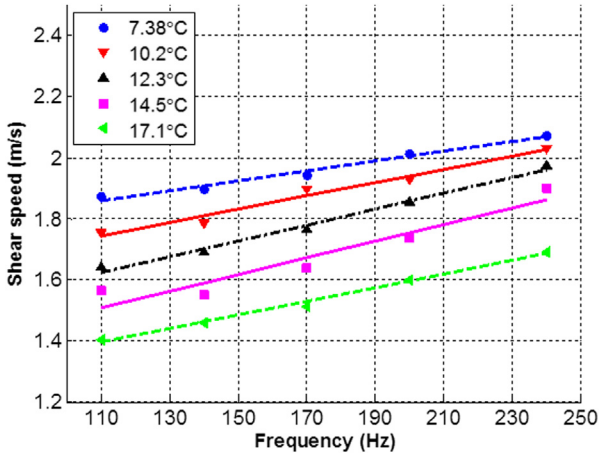

Fig. 2. Shear wave speed estimates in a bovine liver sample versus frequency, obtained at progressively warmer temperatures starting at 7°C. *Solid* and *dashed lines* are linear fits to dispersion data at specific temperatures. The trend is that colder samples are significantly more "stiff" with higher shear wave speed. The general behavior, including dispersion values, is thought to be predicted under the theory of time–temperature superposition, which applies broadly to polymer phantom materials, biomaterials and viscoelastic materials.

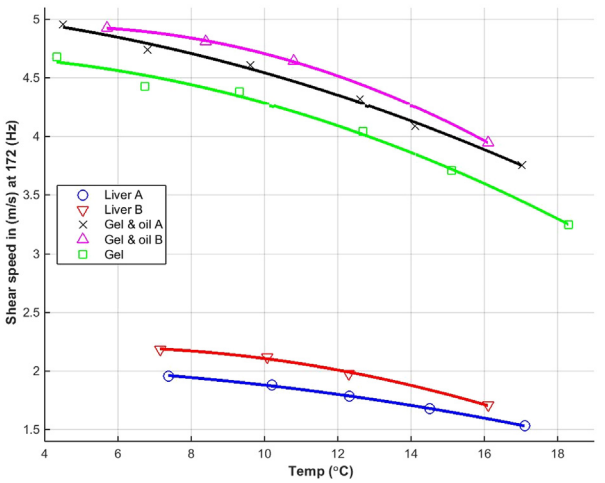

Fig. 3. Shear wave speed in two *ex vivo* beef livers, two gelatin (9.3%) plus castor oil (~20%) phantoms and a pure gelatin (9.3%) phantom. For each temperature in a given sample, the shear speed is taken at the midband frequency of 172 Hz. The *solid lines* represent a second-order polynomial fit where speed c (m/s) is a function of temperature T (°C). Liver A corresponds to the dispersion data illustrated in Figure 2. The second-order polynomial fit for liver A is $c(T) = 2.05 + 0.0012T - 0.0019T^2$.

(2) and (3) for lean and steatotic livers. The independence of the two parameters is an important consideration because it provides the plausibility of dispersion as an independent parameter that could add to the diagnosis of liver steatosis. However, other factors in addition to simple steatosis may affect the measured dispersion. In Figure 1 the highest dispersion values include the steatotic livers from Barry et al. (2012, 2014a), but the next group in descending order includes *in vivo* studies of presumed normal human livers (Deffieux et al. 2009; Muller et al. 2009) and *in vivo* pig livers (Chen et al. 2009).

In studies on humans with varying stages of liver fibrosis, the effects of steatosis have been found to have no clear influence on shear wave speeds in some studies (Bota et al. 2011; Fierbinteanu-Braticevici et al. 2009; Friedrich-Rust et al. 2009; Lupsor et al. 2009; Rifai et al. 2011; Yoneda et al. 2008); however, a few studies reported decreases with increasing steatosis (Fierbinteanu-Braticevici et al. 2013; Yoneda et al. 2010). Furthermore, some specific studies of dispersion slope or viscous models applied to human livers with varying degrees of fibrosis and steatosis have not found a correlation with clinical steatosis grade (Deffieux et al. 2015; Nightingale et al. 2013).

It remains to be seen if other biological effects or the effects of the abdominal wall, present for *in vivo* measurements, or other factors in fibrotic and diseased livers can influence the estimates of dispersion using various techniques.

CONCLUSIONS

A plausible range of dispersion in lean and steatotic livers is established by reviewing existing data around shear wave frequencies of 200 Hz. The important clinical question remains: How much of an increase in dispersion can be expected from the transition from lean to early-stage steatosis in humans? Further studies on animal models and human populations using standardized protocols are required to refine our understanding.

Acknowledgments—This work was supported by the University of Rochester Departments of Electrical & Computer Engineering and Imaging Sciences. The authors are deeply grateful for the many insights and contributions from Dr. Christopher Barry and Professor Edwin Carstensen.

REFERENCES

Angulo P. Nonalcoholic fatty liver disease. N Engl J Med 2002;346: 1221–1231.

Asbach P, Klatt D, Hamhaber U, Braun J, Somasundaram R, Hamm B, Sack I. Assessment of liver viscoelasticity using multifrequency MR elastography. Magn Reson Med 2008;60:373–379.

Barry CT, Hah Z, Partin A, Mooney RA, Chuang KH, Augustine A, Almudevar A, Cao W, Rubens DJ, Parker KJ. Mouse liver dispersion for the diagnosis of early-stage fatty liver disease: A 70-sample study. Ultrasound Med Biol 2014a;40:704–713.

Barry CT, Hazard C, Cheng G, Hah Z, Partin A, Chuang K, Mooney RA, Cao W, Rubens DJ, Parker KJ. Detection of steatosis through shear speed dispersion: A rat study. Presented at the American Institute of Ultrasound in Medicine Annual Convention, Las Vegas, Nevada, 2014b.

Barry CT, Mills B, Hah Z, Mooney RA, Ryan CK, Rubens DJ, Parker KJ. Shear wave dispersion measures liver steatosis. Ultrasound Med Biol 2012;38:175–182.

Bavu E, Gennisson JL, Couade M, Bercoff J, Mallet V, Fink M, Badel A, Vallet-Pichard A, Nalpas B, Tanter M, Pol S. Noninvasive in vivo liver fibrosis evaluation using supersonic shear imaging: A clinical study on 113 hepatitis C virus patients. Ultrasound Med Biol 2011;37:1361–1373.

Blackstock DT. Fundamentals of physical acoustics. New York: Wiley; 2000.

Bota S, Sporea I, Sirli R, Popescu A, Danila M, Sendroiu M. Factors that influence the correlation of acoustic radiation force impulse (ARFI), elastography with liver fibrosis. Med Ultrason 2011;13:135–140.

Boursier J, Isselin G, Fouchard-Hubert I, Oberti F, Dib N, Lebigot J, Bertrais S, Gallois Y, Cales P, Aube C. Acoustic radiation force impulse: A new ultrasonographic technology for the widespread noninvasive diagnosis of liver fibrosis. Eur J Gastroenterol Hepatol 2010; 22:1074–1084.

Carstensen EL, Parker KJ. Physical models of tissue in shear fields. Ultrasound Med Biol 2014;40:655–674.

Chan RW. Estimation of viscoelastic shear properties of vocal-fold tissues based on time-temperature superposition. J Acoust Soc Am 2001;110:1548–1561.

Chen S, Urban MW, Pislaru C, Kinnick R, Zheng Y, Yao A, Greenleaf JF. Shearwave dispersion ultrasound vibrometry (SDUV) for measuring tissue elasticity and viscosity. IEEE Trans Ultrason Ferroelectr Freq Control 2009;56:55–62.

Chen X, Shen YY, Zheng Y, Lin HM, Guo YR, Zhu Y, Zhang XY, Wang TF, Chen SP. Quantification of liver viscoelasticity with acoustic radiation force: A study of hepatic fibrosis in a rat model. Ultrasound Med Biol 2013;39:2091–2102.

Deffieux T, Gennisson JL, Bousquet L, Corouge M, Cosconea S, Amroun D, Tripon S, Terris B, Mallet V, Tanter M, Pol S. Investigating liver stiffness and viscosity for fibrosis, steatosis and activity staging using shear wave elastography. J Hepatol 2015;62:317–324.

Deffieux T, Montaldo G, Tanter M, Fink M. Shear wave spectroscopy for quantification of human soft tissues visco-elasticity. IEEE Trans Med Imaging 2009;28:313–322.

Doyley MM, Perreard I, Patterson AJ, Weaver JB, Paulsen KM. The performance of steady-state harmonic magnetic resonance elastography when applied to viscoelastic materials. Med Phys 2010;38: 3970–3979.

Dyson JK, Anstee QM, McPherson S. Non-alcoholic fatty liver disease: A practical approach to diagnosis and staging. Frontline Gastroenterol 2014;5:211–218.

Einspruch NG, Witterholt EJ, Truell R. Scattering of a plane transverse wave by a spherical obstacle in an elastic medium. J Appl Phys 1960; 31:806–818.

Ferraioli G, Tinelli C, Dal Bello B, Zicchetti M, Filice G, Filice C, Liver Fibrosis Study Group. Accuracy of real-time shear wave elastography for assessing liver fibrosis in chronic hepatitis C: A pilot study. Hepatology 2012;56:2125–2133.

Fierbinteanu-Braticevici C, Andronescu D, Usvat R, Cretoiu D, Baicus C, Marinoschi G. Acoustic radiation force imaging sonoelastography for noninvasive staging of liver fibrosis. World J Gastroenterol 2009;15:5525–5532.

Fierbinteanu-Braticevici C, Sporea I, Panaitescu E, Tribus L. Value of acoustic radiation force impulse imaging elastography for noninvasive evaluation of patients with nonalcoholic fatty liver disease. Ultrasound Med Biol 2013;39:1942–1950.

Fitzpatrick R. Oscillations and waves: An introduction. Boca Raton, FL: Taylor & Francis; 2013. p. 167–208.

Friedrich-Rust M, Wunder K, Kriener S, Sotoudeh F, Richter S, Bojunga J, Herrmann E, Poynard T, Dietrich CF, Vermehren J, Zeuzem S, Sarrazin C. Liver fibrosis in viral hepatitis: Noninvasive

assessment with acoustic radiation force impulse imaging versus transient elastography. Radiology 2009;252:595–604.
Graff KF. Wave motion in elastic solids. Oxford: Clarendon Press; 1975. p. 283–288.
Hah Z, Partin A, Zimmerman G, Parker KJ, Barry CT, Mooney RA, Rubens DJ. Shear wave dispersion measures fat concentration in a mouse liver model. Presented at Eleventh International Conference on the Ultrasonic Measurement of Tissue Elasticity, 2012.
Huwart L, Sempoux C, Salameh N, Jamart J, Annet L, Sinkus R, Peeters F, ter Beek LC, Horsmans Y, Van Beers BE. Liver fibrosis: Noninvasive assessment with MR elastography versus aspartate aminotransferase-to-platelet ratio index. Radiology 2007;245: 458–466.
Huwart L, Sempoux C, Vicaut E, Salameh N, Annet L, Danse E, Peeters F, ter Beek LC, Rahier J, Sinkus R, Horsmans Y, Van Beers BE. Magnetic resonance elastography for the noninvasive staging of liver fibrosis. Gastroenterology 2008;135:32–40.
Klatt D, Hamhaber U, Asbach P, Braun J, Sack I. Noninvasive assessment of the rheological behavior of human organs using multifrequency MR elastography: A study of brain and liver viscoelasticity. Phys Med Biol 2007;52:7281–7294.
Kruse SA, Smith JA, Lawrence AJ, Dresner MA, Manduca A, Greenleaf JF, Ehman RL. Tissue characterization using magnetic resonance elastography: Preliminary results. Phys Med Biol 2000; 45:1579–1590.
Lam B, Younossi ZM. Treatment options for nonalcoholic fatty liver disease. Ther Adv Gastroenterol 2010;3:121–137.
Liu Z, Bilston L. On the viscoelastic character of liver tissue: Experiments and modelling of the linear behaviour. Biorheology 2000; 37:191–201.
Lupsor M, Badea R, Stefanescu H, Sparchez Z, Branda H, Serban A, Maniu A. Performance of a new elastographic method (ARFI technology) compared to unidimensional transient elastography in the noninvasive assessment of chronic hepatitis C: Preliminary results. J Gastrointest Liver Dis 2009;18:303–310.
Muller M, Gennisson JL, Deffieux T, Tanter M, Fink M. Quantitative viscoelasticity mapping of human liver using supersonic shear imaging: Preliminary in vivo feasibility study. Ultrasound Med Biol 2009;35:219–229.
Nightingale KR, Rouze NC, Wang MH, Rosenzweig SJ, Palmeri ML. 3D elasticity imaging with acoustic radiation force. Proc IEEE Int Ultrason Symp 2013;531–536.
Ong JP, Pitts A, Younossi ZM. Increased overall mortality and liver-related mortality in non-alcoholic fatty liver disease. J Hepatol 2008;49:608–612.
Orescanin M, Insana M. Shear modulus estimation with vibrating needle stimulation. IEEE Trans Ultrason Ferroelectr Freq Control 2010;57: 1358–1367.
Palmeri ML, Wang MH, Dahl JJ, Frinkley KD, Nightingale KR. Quantifying hepatic shear modulus in vivo using acoustic radiation force. Ultrasound Med Biol 2008;34:546–558.
Parker KJ. A microchannel flow model for soft tissue elasticity. Phys Med Biol 2014;59:4443–4457.
Rifai K, Cornberg J, Mederacke I, Bahr MJ, Wedemeyer H, Malinski P, Bantel H, Boozari B, Potthoff A, Manns MP, Gebel M. Clinical feasibility of liver elastography by acoustic radiation force impulse imaging (ARFI). Dig Liver Dis 2011;43:491–497.
Salameh N, Larrat B, Abarca-Quinones J, Pallu S, Dorvillius M, Leclercq I, Fink M, Sinkus R, Van Beers BE. Early detection of steatohepatitis in fatty rat liver by using MR elastography. Radiology 2009;253:90–97.
Salameh N, Peeters F, Sinkus R, Abarca-Quinones J, Annet L, ter Beek LC, Leclercq I, Van Beers BE. Hepatic viscoelastic parameters measured with MR elastography: Correlations with quantitative analysis of liver fibrosis in the rat. J Magn Reson Imaging 2007; 26:956–962.
Sandrin L, Fourquet B, Hasquenoph JM, Yon S, Fournier C, Mal F, Christidis C, Ziol M, Poulet B, Kazemi F, Beaugrand M, Palau R. Transient elastography: A new noninvasive method for assessment of hepatic fibrosis. Ultrasound Med Biol 2003;29: 1705–1713.
Sapin-de Brosses E, Gennisson JL, Pernot M, Fink M, Tanter M. Temperature dependence of the shear modulus of soft tissues assessed by ultrasound. Phys Med Biol 2010;55:1701–1718.
Schreuder TC, Verwer BJ, van Nieuwkerk CM, Mulder CJ. Nonalcoholic fatty liver disease: An overview of current insights in pathogenesis, diagnosis and treatment. World J Gastroenterol 2008;14: 2474–2486.
Wang MH, Palmeri ML, Guy CD, Yang L, Hedlund LW, Diehl AM, Nightingale KR. In vivo quantification of liver stiffness in a rat model of hepatic fibrosis with acoustic radiation force. Ultrasound Med Biol 2009;35:1709–1721.
Wanless IR, Lentz JS. Fatty liver hepatitis (steatohepatitis) and obesity: An autopsy study with analysis of risk factors. Hepatology 1990;12: 1106–1110.
White RM. Elastic wave scattering at a cylindrical discontinuity in a solid. J Acoust Soc Am 1958;30:771–785.
Wu Z, Taylor LS, Rubens DJ, Parker KJ. Sonoelastographic imaging of interference patterns for estimation of the shear velocity of homogeneous biomaterials. Phys Med Biol 2004;49:911–922.
Xie H, Shamdasani V, Fernandez AT, Peterson R, Lachman M, Yan S, Robert J, Urban M, Shigao C, Greenleaf J. Shear wave dispersion ultrasound vibrometry (SDUV) on an ultrasound system: in vivo measurement of liver viscoelasticity in healthy animals. Proc IEEE Int Ultrason Symp 2010;912–915.
Yin M, Talwalkar JA, Glaser KJ, Manduca A, Grimm RC, Rossman PJ, Fidler JL, Ehman RL. Assessment of hepatic fibrosis with magnetic resonance elastography. Clin Gastroenterol Hepatol 2007;5: 1207–1213.
Yoneda M, Suzuki K, Kato S, Fujita K, Nozaki Y, Hosono K, Saito S, Nakajima A. Nonalcoholic fatty liver disease: US-based acoustic radiation force impulse elastography. Radiology 2010;256: 640–647.
Yoneda M, Yoneda M, Mawatari H, Fujita K, Endo H, Iida H, Nozaki Y, Yonemitsu K, Higurashi T, Takahashi H, Kobayashi N, Kirikoshi H, Abe Y, Inamori M, Kubota K, Saito S, Tamano M, Hiraishi H, Maeyama S, Yamaguchi K, Togo S, Nakajima A. Noninvasive assessment of liver fibrosis by measurement of stiffness in patients with nonalcoholic fatty liver disease (NAFLD). Dig Liver Dis 2008;40:371–378.
Zhang M, Castaneda B, Wu Z, Nigwekar P, Joseph JV, Rubens DJ, Parker KJ. Congruence of imaging estimators and mechanical measurements of viscoelastic properties of soft tissues. Ultrasound Med Biol 2007;33:1617–1631.